

ARTICLE

OPEN



Activation of FXR and inhibition of EZH2 synergistically inhibit colorectal cancer through cooperatively accelerating FXR nuclear location and upregulating CDX2 expression

Junhui Yu¹, Kui Yang¹, Jianbao Zheng¹, Pengwei Zhao¹, Jie Xia¹ ² , Xuejun Sun¹ and Wei Zhao¹

© The Author(s) 2022, corrected publication 2023

Our previous study indicated that colon cancer cells varied in sensitivity to pharmacological farnesoid X receptor (FXR) activation. Herein, we explore the regulatory mechanism of FXR in colorectal cancer (CRC) development and aim to design effective strategies of combined treatment based on the regulatory axis. We found that the expression of FXR was negatively correlated with enhancer of zeste homolog 2 (EZH2) in colon cancer tissues. EZH2 transcriptionally suppressed FXR via H3K27me3. The combination of FXR agonist OCA plus EZH2 inhibitor GSK126 acted in a synergistic manner across four colon cancer cells, efficiently inhibiting clonogenic growth and invasion in vitro, retarding tumor growth in vivo, preventing the G0/G1 to S phase transition, and inducing caspase-dependent apoptosis. Benign control cells FHC were growth-arrested without apoptosis induction, but retained long-term proliferation and invasion capacity. Mechanistically, the drug combination dramatically accelerated FXR nuclear location and cooperatively upregulated caudal-related homeobox transcription factor 2 (CDX2) expression. The depletion of CDX2 antagonized the synergistic effects of the drug combination on tumor inhibition. In conclusion, our study demonstrated histone modification-mediated FXR silencing by EZH2 in colorectal tumorigenesis, which offers useful evidence for the clinical use of FXR agonists combined with EZH2 inhibitors in combating CRC.

Cell Death and Disease (2022)13:388; <https://doi.org/10.1038/s41419-022-04745-5>

INTRODUCTION

Colorectal cancer (CRC) ranks the third commonly diagnosed cancer globally, which caused approximately 935,000 death every year. Most CRC patients are diagnosed at the advanced stage due to insidious symptoms in the early stage [1, 2]. Despite the great progress has been achieved in multimodality therapy for CRC, the prognosis of advanced-stage CRC is still poor. The five-year survival rate of stage IV CRC patients is slightly higher than 10% [3]. Hence, clarification of pivotal genes and their regulatory mechanisms during colorectal tumorigenesis is urgently required for developing innovative and effective strategies in confronting CRC.

CRC is a multifactorial disease involving both hereditary and environmental factors.

Multiple risk factors for CRC include obesity, physical inactivity, poor diets, alcohol drinking, and smoking [4]. More importantly, many mutations in genes, e.g., APC, TP53, SMAD4, PIK3CA, and KRAS, copy-number changes, chromosomal translocation patterns, and myc-directed transcriptional activation or repression contribute to colorectal tumorigenesis [5]. The complex and heterogeneous genetic characteristics of CRC hinder the discovery of universal molecular targets, and the effectiveness of subsequent targeted therapies.

Epidemiological studies, animal models, and clinical studies identify fecal bile acid as a risk factor for colon cancer [6]. High levels of bile acids elicit hazardous influence on colonic mucosa characterized by DNA oxidative damage [7], inflammation [8], and hyperproliferation [9]. Farnesoid X receptor (FXR, translated by the NR1H4 gene), a bile acid-activated nuclear receptor, regulates the expression of target genes involved in lipid, cholesterol, and glucose metabolism [10]. Emerging evidence supports the pivot role of FXR in tumorigenesis. The deficiency of FXR correlates with tumor progression and often signifies adverse clinical outcomes [11]. Recently, obeticholic acid (OCA), a novel FXR agonist, preliminarily exhibits a tumor inhibitory activity in CRC [12], hepatocellular carcinoma (HCC) [13], and cholangiocarcinoma [14]. However, the complex regulatory network of FXR in tumor might hamper the implementation of FXR agonist in clinical treatment [15]. We previously demonstrated that the antiparasitic drug nitazoxanide (NTZ) acted synergistically with OCA in tumor inhibition by abrogating β -Catenin expression [16]. GW4064, an FXR agonist, combined with acyclic retinoid (ACR), exerted synergistic inhibitory effects on the growth of HCC with lower doses of both agents [17]. Generally, epigenetic aberrations including DNA methylation, chromatin remodeling, and histone modification contribute to tumorigenesis by dysregulating the

¹Department of General Surgery, First Affiliated Hospital of Xi'an Jiaotong University, 710061 Xi'an, PR China. ²State Key Laboratory of Bioactive Substance and Function of Natural Medicines, Department of New Drug Research and Development, Institute of Materia Medica, Chinese Academy of Medical Sciences and Peking Union Medical College, 100050 Beijing, PR China. email: jiexia@imm.ac.cn; sunxy@mail.xjtu.edu.cn; zhaowei9803@126.com

Received: 26 July 2021 Revised: 9 February 2022 Accepted: 18 March 2022
Published online: 21 April 2022

transcriptional activity [18]. Herein, the epigenetic regulatory mechanism of FXR in colorectal tumorigenesis is deeply explored.

Enhancer of zeste homolog 2 (EZH2), a member of polycomb-repressive complex 2 (PRC2) complex, regulates the expression of target genes by catalyzing trimethylation of lysine 27 on histone H3 (H3K27me3) [19]. Due to the selectivity of PRC2-mediated gene silencing, EZH2 functions oncogenic or tumor-suppressive role in human malignancies. In CRC tissues, EZH2 expression is significantly elevated and often correlates with poor prognosis [20, 21]. Importantly, targeting EZH2 could significantly enhance death receptors and reduce tumorigenic potential of CRC *in vivo* and *in vitro* [22], supporting EZH2 as a promising therapeutic target.

In the present study, we aim to explore the epigenetic modification of FXR in CRC, and design innovative and effective strategies of combined treatment based on the identified regulatory axis.

MATERIALS AND METHODS

Cell cultures

Colon cancer cells HT-29, HCT116, SW403, SW480, SW620, RKO, HT-29, and DLD-1 and normal colon epithelial cells FHC (Shanghai Institute of Cell Biology, Chinese Academy of Sciences) were all routinely cultured in DMEM supplemented with 10% fetal bovine serum (FBS) at 5% CO₂ at 37 °C. Once the cells reached 70% confluence, they were treated with various doses of OCA for 48 h along with GSK126.

Bioinformatic analysis

Bioinformatic analysis is conducted via the TCGA database and NCBI Gene Expression Omnibus (GEO, <https://www.ncbi.nlm.nih.gov/gds/>) under accession numbers (GSE8023)

Lentiviral vectors and transfection

Lentiviral vectors with EZH2/FXR shRNA or overexpression were purchased from GeneChem Co., Ltd. (Shanghai, China). All transfections were performed according to the manufacturer's instructions.

Drug combination studies

Cells per well were seeded in the 96-well plates at a density of 5×10^3 , and then treated with a single compound or with a combination of OCA and GSK126 for another 48 h. Cell viability was measured using the CCK-8 assay [23]. Combination index (CI) and fraction affected (Fa) values were calculated using Compusyn software. CI > 1 indicates antagonism, CI = 1 indicates an additive effect, and CI < 1 indicates synergy.

CCK8, colony formation, cell cycle, and apoptosis assays

CCK8 assays were performed as described previously [23]. For colony formation assay, three hundred cells were seeded and cultured for 14 days. Colonies (≥ 50 cells/colony) were counted. Cell cycle distributions were evaluated by flow cytometry as previously described [23]. For apoptosis assay, cells were labeled with Annexin V PE/7-AAD (BD Biosciences, Franklin Lakes, NJ, USA) according to the manufacturer's protocol as previously described [24]. Each experiment was performed in triplicate.

Wound-healing assays

Cells were cultured in six-well plates until 90% confluence. Pipette tips (10 μ L) were then utilized to scratch artificial vertical lines. The cells were maintained in FBS-free medium for an additional 48 h. The images of wound closure were captured under a microscope at 0 and 48 h.

Transwell assays

Cell invasion was measured by using Transwell plates (Corning, New York, NY, USA) with Matrigel (BD, Franklin Lakes, NJ, USA). The lower chamber was filled with 600 μ L of DMEM containing 20% FBS. The upper chamber filters were pre-coated with 50 μ L of Matrigel and plated at 10×10^4 cells per upper chamber. The cells were incubated at 37 °C for 48 h. After incubation, non-migratory cells on the upper surface of the Transwell inserts were removed by washing with fresh phosphate buffered

solution (PBS). The migratory or invading cells on the underside of the membrane were fixed with 4% paraformaldehyde and stained with 1% crystal violet. The number of cells was counted in three randomly selected fields of fixed cells under an inverted microscope. Each experiment was performed in triplicate.

Nude mouse xenograft assay

All animal experiments were performed in accordance with the institutional guidelines, and were approved by the Laboratory Animal Center of Xi'an Jiaotong University. The 5 week-old female BALB/c-nude mice was purchased from Shanghai SLAC Laboratory Animal Co., Ltd. (Shanghai, China). The mice were injected with 5×10^6 colon cancer cells into the right flanks to establish xenograft tumor model. Once the size of xenograft tumors reached approximately 100 mm³, the nude mice were randomly divided into four subgroups, each consisting of five mice and were administered by oral gavage of OCA (10 mg/kg/day) and GSK126 (50 mg/kg/day) alone or in combination for consecutive 18 days. Tumor size was monitored using callipers every 3 days, and the tumor volume was measured according to the formula ($a \times b^2 \times 0.5$, a : length, b : width). After 18 days of drug administration, the mice were executed and the xenograft tumors were isolated and weighted.

RNA isolation and real-time PCR

RNA isolation, complementary DNA (cDNA) synthesized, and real-time PCR were performed as described previously [23]. The sequences of primers were summarized in Supplementary Table 1. Each experiment was performed in triplicate.

Immunohistochemistry (IHC)

The protocol was performed as previously described [23]. Briefly, the extent of stained cells (0, 0–5%; 1, 6–25%; 2, 26–50%; 3, 51–75%; and 4, 76–100%) and the staining intensity (0, negative; 1, light brown; 2, brown; and 3, dark brown) were recorded. The immunoreactivity scores (IRSs) were defined as the product of extent and intensity scores. An IRS of >3 was considered as positive expression.

Total protein extraction and Western blot

The detailed protocol was performed as described previously [23]. The antibody information was presented in Supplementary Table 2. Each experiment was performed in triplicate.

Immunofluorescence (IF)

The cells were fixed with 4% paraformaldehyde for 20 min and permeabilized with 0.2% Triton X-100 for 10 min. After blocking with 5% bovine serum albumin (BSA) for 30 min at room temperature, the cells were incubated at 4 °C overnight with primary antibodies against FXR or β -Catenin (1:100 dilution). The dishes were washed three times with PBS for 10 min each and then incubated with Alexa Fluor 594/488-conjugated secondary antibodies (1:400 dilution, Invitrogen, Carlsbad, CA, USA) for 1 h at room temperature. The nuclei were stained with DAPI (10 mg/ml) for 10 min. The samples were examined via microscopy (Leica Microsystems, Heidelberg, Germany) to analyze the subcellular localization of FXR and β -Catenin.

Luciferase reporter assay

For promoter analyses, a fragment of the CDX2 5'-flanking sequence (from –1059 bp to +89 bp) and other truncated fragments were cloned into the pGL3.0 Basic Vector (Promega, Madison, WI, USA) to generate a CDX2 full promoter reporter construct and the truncated ones (Supplementary Table 1). The plasmids containing firefly luciferase reporters of CDX2 promoter and the truncated ones, and the pTK-RL plasmids were co-transfected into cells. The detailed protocol was carried out as described previously [23].

Quantitative chromatin immunoprecipitation (qChIP)

Cells were subjected to ChIP using the EZ-ChIP Kit (Millipore, Bedford, MA, USA).

The detailed protocol was performed as described previously [23]. Real-time PCR was conducted to amplify the regions of DNA fragments by using special primers (Supplementary Table 1). Each experiment was performed in triplicate.

Statistical analysis

The differences among the groups were compared by the Student's *t*-test or one-way ANOVA. All statistical analyses were performed using the SPSS statistical package (SPSS Inc., Chicago, IL, USA). $P < 0.05$ was considered statistically significant.

RESULTS

FXR expression is transcriptionally suppressed by EZH2 via H3K27me3

Previous studies indicated that FXR deficiency confers poor prognosis of patients with several cancer types [11, 14, 25], which was further confirmed in colon cancer patients in our previous study [26]. Restoration of FXR significantly suppressed aggressive behavior of colon cancer [26]. The pivotal role of FXR in CRC onset highlights the importance to elucidate the regulatory mechanisms of FXR. Intriguingly, analysis of GEO database (GSE8023) revealed that treatment of LnCaP cells with EZH2 inhibitor GSK126 or EPZ-6438 strikingly induced FXR mRNA up-regulation (Fig. 1a). TCGA database mining also supported an inverse correlation between EZH2 and FXR in the patients with colon cancer (Fig. 1b). Hence, we inferred that EZH2 negatively regulated FXR expression in CRC.

We firstly analyzed the protein levels of FXR and EZH2 in eight colon cancer cells by western blotting. FXR is expressed in colon cancer cells at variable levels; however, an inverse correlation was observed between FXR and EZH2 expression (Fig. 1c). HCT116 and RKO cells harboring high EZH2 level were conducted with EZH2 knockdown and SW403 and SW480 with EZH2 deficiency were conducted with EZH2 overexpression. Transfection with EZH2 shRNA lentiviral dramatically increased the levels of FXR in HCT116 and RKO cells (Fig. 1d), while enhancing EZH2 expression led to a decreased level of FXR in SW403 and SW480 cells (Fig. 1e). As expected, GSK126 strikingly elevated the expression of FXR in HCT116 and SW480 cells (Fig. 1f). The analysis from qChIP assay revealed an enrichment of H3K27me3 and EZH2 in the promoter region of FXR (Fig. 1g). Moreover, ectopic expression of EZH2 enhanced the binding of H3K27me3 to FXR upstream region (Fig. 1h).

The clinical correlation between EZH2 and FXR in CRC was explored in the tissue microarrays containing 90 pairs of colon cancer by IHC staining (cohort I, Fig. 2a). The EZH2 level was negatively correlated with FXR (Fig. 2b). Moreover, another independent cohort of 162 colon cancer patients revealed a negative correlation between FXR and EZH2 (Fig. 2c, d). Altogether, these results suggested that EZH2 acts a negative regulator of FXR in CRC through H3K27me3.

FXR transcriptionally activates the expression of tumor suppressor CDX2

We next explored the downstream targets directly regulated by FXR in CRC. Our previous study revealed the regulatory effect of FXR on caudal-related homeobox transcription factor 2 (CDX2), a tumor suppressor, although the precise mechanism is unclear [27]. Intriguingly, bioinformatic analysis of the proximal promoter of CDX2 identified a potential FXR response element, an inverted repeat-1 (IR-1, 5'-AGGTCGCTGCCCT-3'), located -449 to -461 bp upstream of the transcription start site. Hence, we attempted to validate the involvement of CDX2 in FXR-mediated tumor inhibition in CRC. Firstly, CDX2 promoter reporter constructs with full length from -1059 bp to +89 bp or truncated promoter were designed. The dual-luciferase reporter assay indicated that enhancing FXR expression induced an elevation of luciferase activity of constructs with the -1059, -819, or 519 bp to +89 bp region; however, deficiency of -519 bp to -376 bp region abolished this induction (Supplementary Fig. 1a). These data indicated that FXR might bind to the -519 bp to -376 bp region of CDX2 promoter to transactivate CDX2. A qChIP assay was then carried out to identify the special site of FXR binding to CDX2

promoter. This fragment corresponding to IR-1 element was enhanced upon FXR overexpression (Supplementary Fig. 1b). Meanwhile, in relation to the single drug, OCA and GSK126 combination dramatically enhanced the binding of FXR to the IR-1 element in CDX2 promoter region (Supplementary Fig. 1c).

Furthermore, ectopic expression of FXR led to an up-regulation of CDX2 levels in SW403 and SW480 cells (Supplementary Fig. 1d, e). Conversely, FXR depletion in HCT116 and RKO cells decreased CDX2 levels (Supplementary Fig. 1f, g). Collectively, our study indicated that FXR transcriptionally activates the expression of tumor suppressor CDX2.

Inhibition of EZH2 acts synergistically activation of FXR with in colon cancer cells

We previously reported that that colon cancer cells exhibited the varying responses to FXR agonist OCA [16]. Based on IC_{50} values, cells were clearly divided into two groups with low and high sensitivity (Supplementary Fig. 2a). IC_{50} values of RKO and HCT116 cells were below 1 μ M in the high-sensitive group, but well above 4 μ M in the low sensitive group with SW403 and SW480 cells. Normal colon epithelial cells FHC reacted to OCA at low concentration (IC_{50} 0.34 μ M). In the present study, the regulation of FXR by EZH2 renders us to speculate that EZH2 inhibition enhances the therapeutic effect of FXR agonist OCA against CRC.

We firstly assessed the IC_{50} values of colon cancer cells and FHC cells response to EZH2 inhibitor GSK126. The results indicated that GSK126 inhibited the growth of HCT116, SW403, SW480, RKO, and FHC cells with IC_{50} values of approximately 3.347, 6.155, 4.378, 3.718, and 0.611 μ M, respectively (Supplementary Fig. 2a). The extent of synergism of GSK126 combined with OCA was analyzed by combination index (CI) from CompuSyn software. Strong synergisms were observed in four colon cancer cells (Supplementary Fig. 2c-f). Intriguingly, the strongest synergies were seen in the low OCA-sensitive SW480 and SW403 cells (Supplementary Fig. 2e, f). Conversely, a limited synergistical effect was found in normal colon epithelial cells FHC (Supplementary Fig. 2b). Altogether, this evidence suggests that EZH2 inhibitor might enhance the efficacy of FXR agonist against CRC.

FXR agonist and EZH2 inhibitor synergistically inhibit colon cancer cell proliferation and migration

We then carried out a series of in vitro experiments to evaluate the synergistical effect of OCA combined with GSK126. RKO, SW403, SW480, HCT116, and FHC cells were treated with OCA and GSK126 alone or in combination. Dosages of combined treatment were adopted from synergistic combinations and blow the IC_{50} of the two drugs. Firstly, in relation to the single drug, OCA and GSK126 combination consistently repressed colony-forming ability of four colon cancer cells (Fig. 3a). Notably, no remarkable clonogenic growth was seen in FHC cells. Next, we analyzed cell cycle distribution of cells exposure to OCA and GSK126 combination by flow cytometry. The combined treatment induced the proportion of cells at G0/G1 phase with the decreased proportion in S phase in four colon cancer cells (Fig. 3b). FHC cells exhibited an arrest in G0/G1 with a reduction of the S-phase and G2/M fractions. Moreover, a remarkable upregulation of the apoptosis rate was induced in four colon cancer cells, but not FHC cells, upon combined treatment (Fig. 3c). Finally, combination treatment dramatically attenuated the invasive and migratory potential of four colon cancer cells (Fig. 3d-e). No significant alteration of invasion and migration was observed in FHC cells.

Consistently, the protein levels of cell cycle- and invasion-related genes were dramatically altered upon combined treatment (Supplementary Fig. 3a, b). Altogether, this evidence suggests that EZH2 inhibition enhances the therapeutic effect of FXR agonist OCA against CRC.

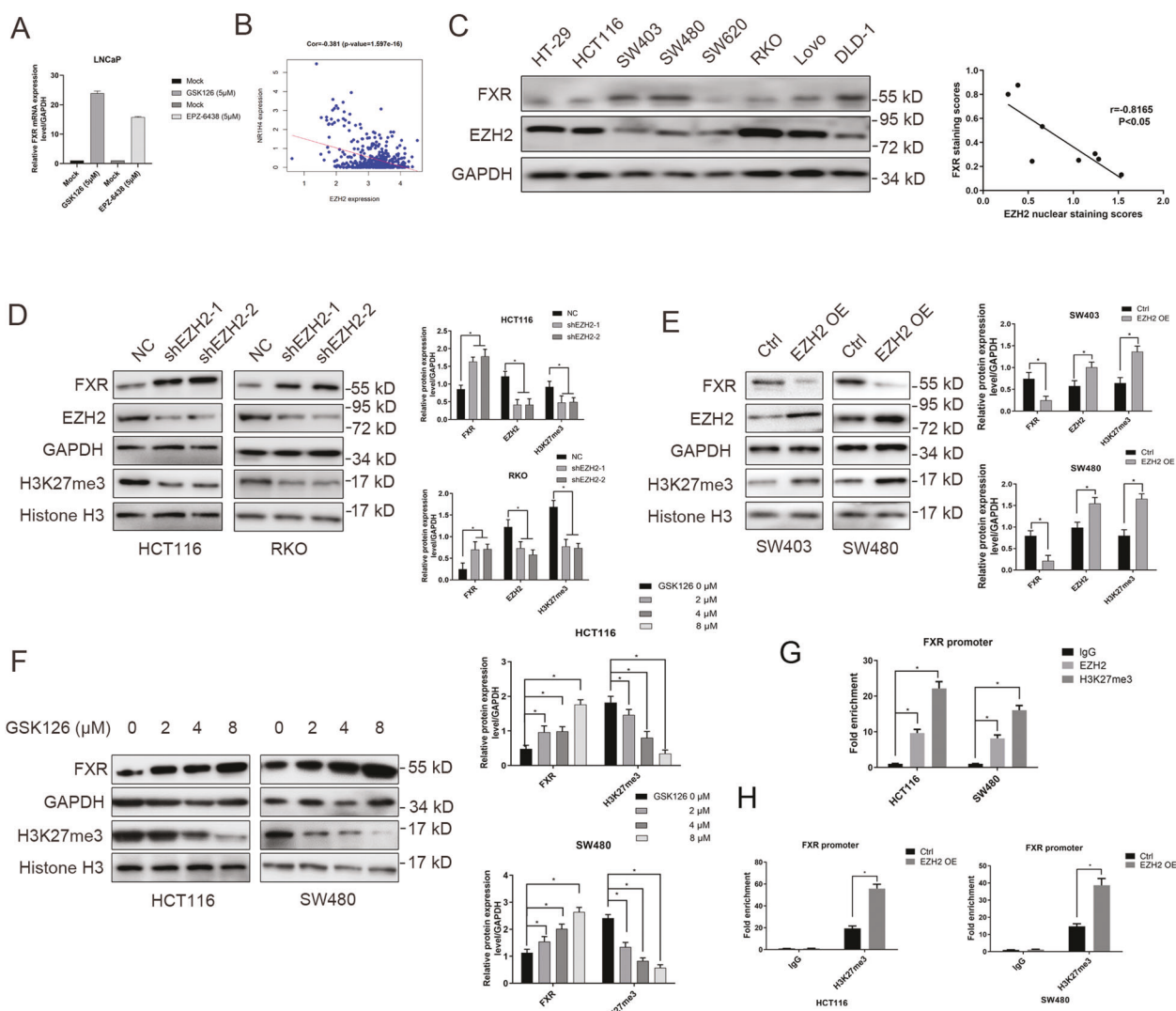


Fig. 1 EZH2 negatively regulated the expression of FXR by H3K27me3. **a** Relative NR1H4 mRNA levels in LNCaP cells treated or not with GSK126. **b** Correlation analysis of EZH2 and FXR mRNA level in colon cancer tissues from TCGA database. **c** The protein levels of EZH2 and FXR in colon cancer cells by western blotting analysis (left panel: gel bands; right panel: correlation analysis between EZH2 and FXR). **d** The protein levels of FXR and H3K27me3 in HCT116 and RKO cells with EZH2 depletion by western blotting analysis (left panel: gel bands; right panel: quantitative analysis of these proteins). **e** The protein levels of FXR and H3K27me3 in SW403 and SW480 cells with EZH2 overexpression by western blotting analysis (left panel: gel bands; right panel: quantitative analysis of these proteins). **f** The effect of EZH2 inhibitor GSK126 on the protein levels of FXR and H3K27me3 in SW403 and SW480 cells by western blotting analysis (left panel: gel bands; right panel: quantitative analysis of these proteins). **g** The ChIP analysis of the enrichment of H3K27me3 and EZH2 in the FXR promoter region. **h** The effect of enhancing EZH2 expression on the enrichment of H3K27me3 to in the FXR promoter region. All data are the mean \pm SD of three independent experiments. * P < 0.05.

FXR agonist and EZH2 inhibitor synergistically inhibits the tumorigenesis of colon cancer cells through cooperatively accelerating FXR nuclear location and upregulating CDX2 expression

FXR agonist OCA performs its function by accelerating FXR nuclear translocation and occupancy of its target genes [28]. Meanwhile, our study found that treatment with EZH2 inhibitor GSK126 elevated the expression of FXR. Hence, we assumed that whether the synergistic inhibitory effects of GSK126 and OCA might be related to the accelerative nuclear localization of FXR. As expected, the results from western blotting analysis indicated that OCA dramatically expedited nuclear localization of FXR, which level was enhanced upon GSK126 treatment (Fig. 4a). IF assays also indicated that the combination of GSK126 and OCA expedited the nuclear localization of FXR compared to the single drug (Fig. 4b). Moreover, the role of FXR target gene, CDX2, under

GSK126 and OCA treatment was investigated. In HCT116 and RKO cells, addition of GSK126 and OCA alone effectively elevated the expression of CDX2, while the effect was much stronger under the combined treatment (Fig. 4a). Importantly, CDX2 depletion greatly blocked the inhibitory effects of GSK126 and OCA on the proliferation and invasion of colon cancer cells (Fig. 4c–g).

Consequently, the signaling pathways regulated by CDX2 were further investigated when administering a combined GSK126 and OCA treatment. Our previous studies demonstrated that CDX2 retarded Akt and GSK-3 β phosphorylation, and thereby inhibited β -Catenin nuclear translocation [29]. In HCT116 and SW480 cells, the combination of GSK126 and OCA synergistically retarded the phosphorylation of Akt (Ser473) and GSK-3 β (Ser9) and decreased nuclear β -Catenin protein levels compared to the single drug (Fig. 5a); meanwhile, CDX2 depletion antagonized this effect under the combined treatment (Fig. 5c). Overexpression of FXR

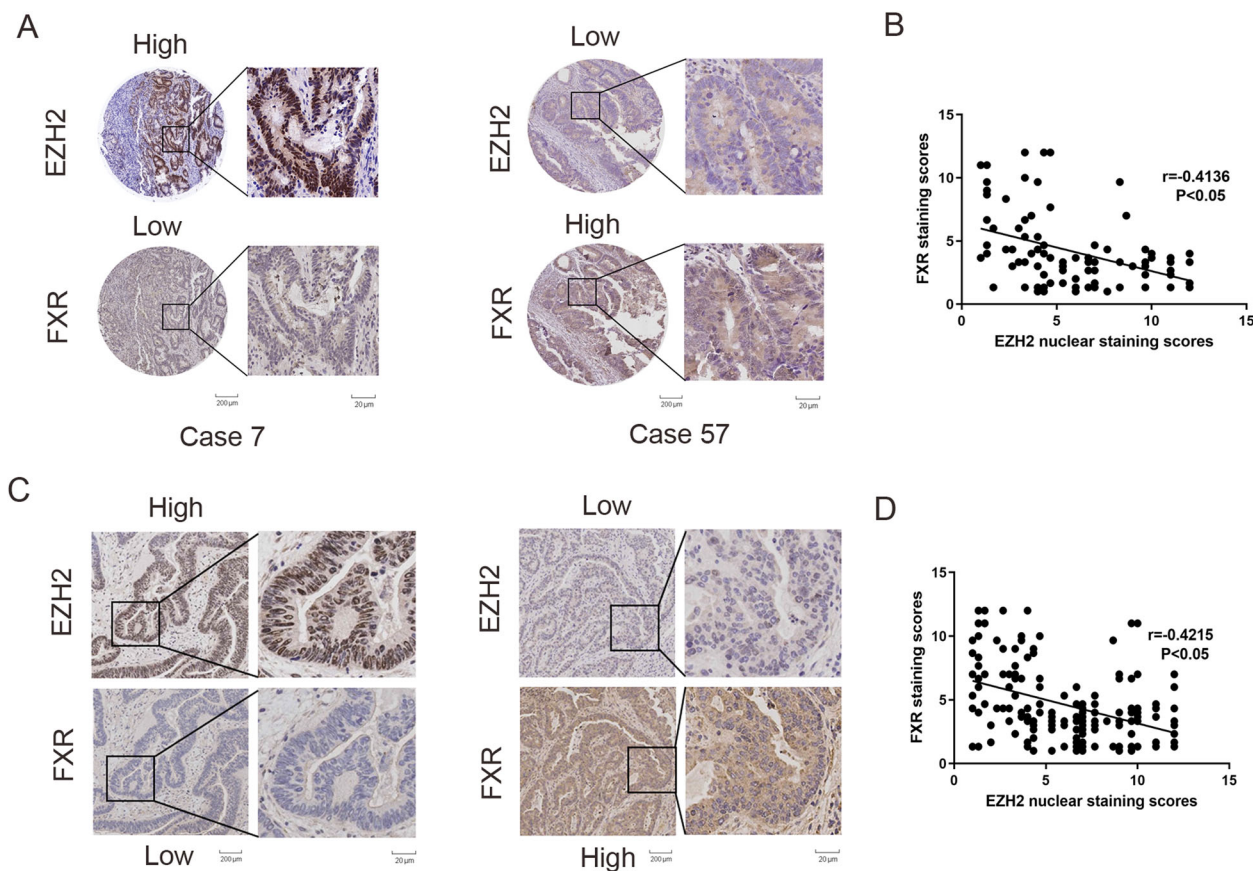


Fig. 2 An inverse correlation between EZH2 and FXR was found in the patients with colon cancer. **a** EZH2 and FXR expression in tissue microarrays purchased from Shaanxi Kexin Biotechnology Co., Ltd, including 90 pairs of CRC samples and paired NC tissues by IHC staining (cohort I). **b** Correlation analysis of EZH2 and FXR in CRC tissue microarrays. **c** EZH2 and FXR expression in an independent cohort of 403 colon cancer tissues sample from at the First Affiliated Hospital of Xi'an Jiaotong University by IHC staining (cohort II). **d** Correlation analysis of EZH2 and FXR in 403 colon cancer tissues microarrays. All data are the mean \pm SD of three independent experiments. $*P<0.05$.

and knockdown of EZH2 achieved the comparable effects (Fig. 5b), which was abrogated by CDX2 (Fig. 5d). Furthermore, the TOP/FOP-Flash reporter assay indicated that, relative to the single drug treatment, the combination of OCA and GSK126 or overexpression of FXR and knockdown of EZH2 synergistically inhibited TCF/LEF transcriptional activities (Supplementary Fig. 4a, b), which was abrogated by CDX2 knockdown (Supplementary Fig. 4c, d). The results from IF assays indicated that the combination of GSK126 and OCA synergistically suppressed the nuclear translocation of β -Catenin, and this effect was attenuated by CDX2 depletion (Fig. 5e). Importantly, knockdown of CDX2 restored the protein levels of cell cycle- and invasion-related genes under combined treatment with OCA and GSK126 (Fig. 5f). Taken together, these data suggested that inhibition of EZH2 and activation of FXR synergistically accelerated FXR nuclear localization and promoted the expression of CDX2 and its regulated signaling pathways.

FXR agonist and EZH2 inhibitor synergistically suppresses growth of CRC in vivo

To validate the synergy of OCA and GSK126 in tumor growth suppression in vivo, nude mice with subcutaneous xenograft formed by HCT116 and SW480 cells were treated with OCA and GSK126 alone or in combination (Fig. 6a, e). Combined treatment dramatically retarded tumor growth curve and lessened tumor weight relative to the single drug treatment (Fig. 6b, d, f, h). Q value analyzed from Zhengjun Jin method for HCT116 and SW480 xenografts is 1.07 and 1.10, respectively [30], implying a synergistical effect of the combination treatment. Notably, the progression-free survival (PFS) of nude mice in combined

treatment group is remarkably lengthened (Fig. 6c, g). Mechanistically, combination treatment results in a stronger staining of CDX2, p21, active caspase-3, and E-cadherin, and a weaker staining of MMP-9. Collectively, combination of OCA and GSK126 display strong synergy in tumor growth inhibition in vivo.

DISCUSSION

Chemotherapy based on fluorouracil for CRC is below expectation and limited by drug resistance and side effects. Monotargeted therapies are novel and alternative treatment options that have brought about widespread attention. However, the complicated signaling networks and tumor heterogeneity hinder the implement of these drugs [31]. Recently, combination therapy has gathered tremendous interest with its ability to enhance efficacy and reduce side effects. In the present study, we demonstrated that EZH2 transcriptionally suppressed FXR expression via H3K27me3, which subsequently elevated the expression of tumor suppressor gene CDX2 and its regulatory pathways. Accordingly, the combination of EZH2 inhibitor (GSK126) and FXR agonist (OCA) synergistically elicited the antitumor activity in CRC.

FXR, a member of the nuclear receptor superfamily, is widely expressed in liver, intestine, and kidneys [32, 33]. Emerging evidence supports the involvement of FXR in human tumorigenesis. FXR plays a causative role in pancreatic [34] and esophageal [35] carcinomas. On the other hand, mice with FXR-deficiency are vulnerable to developing HCC [36]. The lack of FXR triggered intestinal inflammation and eventually promote colon tumorigenesis [11]. Conversely, restoration of FXR repressed intestinal cell

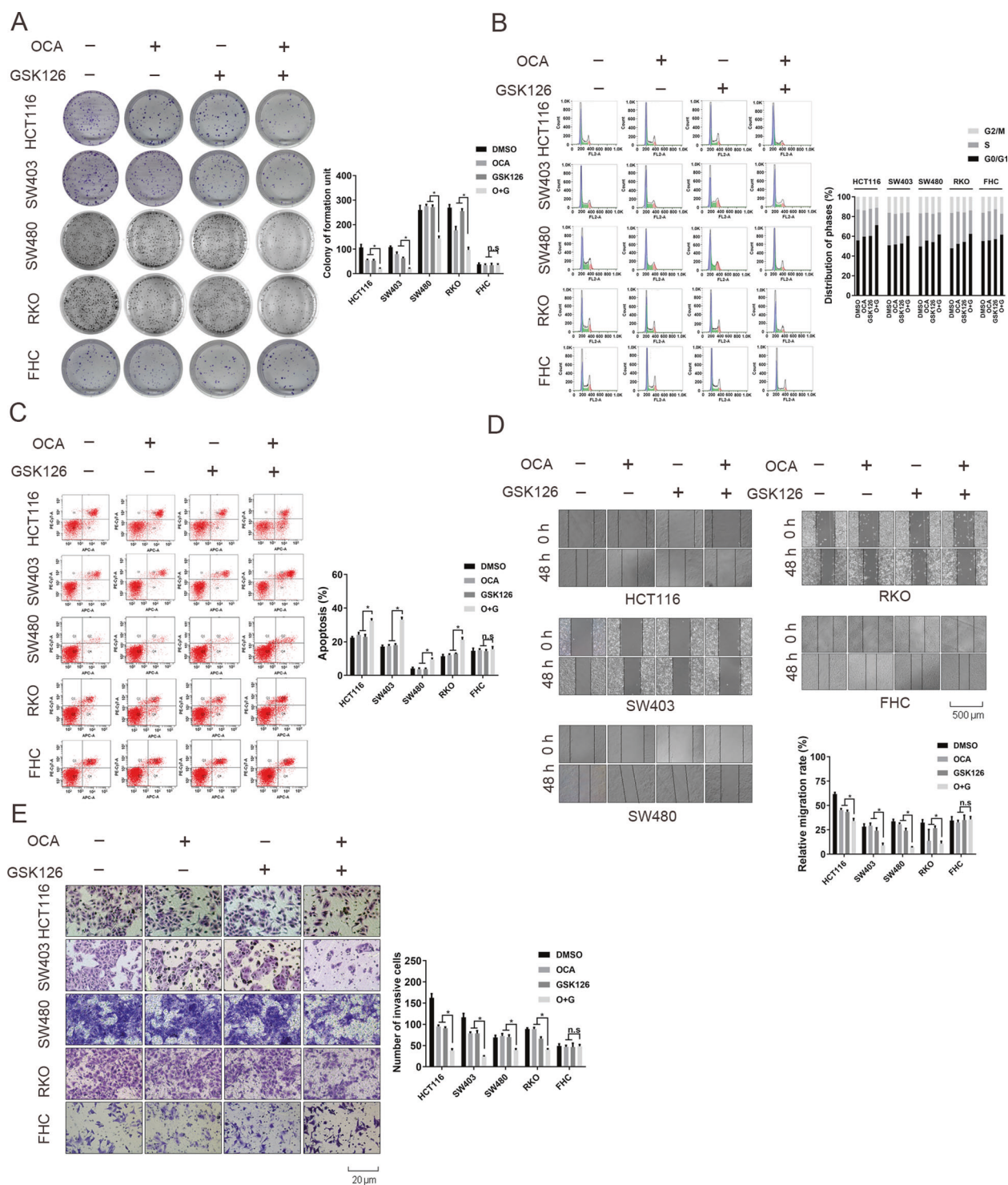


Fig. 3 OCA and GSK126 synergistically inhibited the tumorigenic properties of colon epithelial cells in vitro. **a-c** The effect of OCA, GSK126 alone, or OCA plus GSK126 on colony formation (a left panel: colony formation assays; right panel: quantitation of the data), cell cycle distribution (b left panel: cell cycle analysis assays; right panel: quantitation of the data), and apoptosis (c left panel: apoptosis assays; right panel: quantitation of the data) of colon epithelial cells. **d, e** The effect of OCA, GSK126 alone or OCA plus GSK126 on the migration (d up panel: wound-healing assays; down panel: quantitation of the data) and invasion (e left panel: transwell assays; right panel: quantitation of the data) of colon epithelial cells. All data are the mean \pm SD of three independent experiments. * $P < 0.05$.

growth and blocked CRC progression [37]. Mechanistically, FXR antagonized Wnt/β-Catenin signaling by forming a complex with β-Catenin [26]. The FXR/β-Catenin complex in turn hinders FXR-mediated transcriptional activation of target gene SHP [26]. Despite of the involvement of FXR in onset and progression of

several types of cancer, the regulatory mechanism of its expression is obscure. Hence, we observed a negative clinical correlation between FXR and EZH2 expression in colon cancer tissues. EZH2 promotes transcriptional silencing by methylating histone methyltransferase H3K27 [38]. Increasing evidence

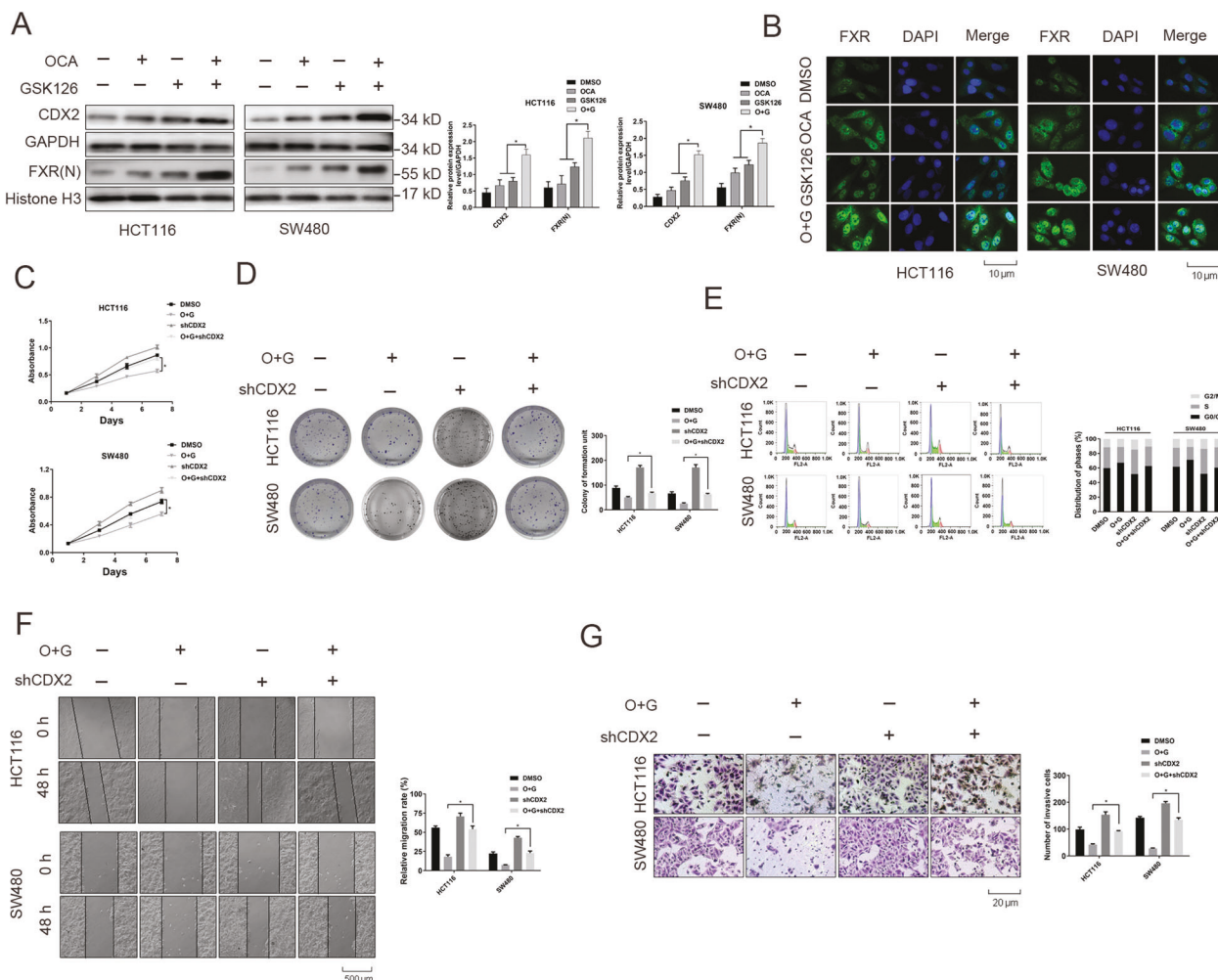


Fig. 4 The depletion of CDX2 antagonized the synergistic effects of the combination of OCA and GSK126 on tumor inhibition. a The protein levels of CDX2 and FXR (nuclear) in HCT116 and SW480 cells treated with OCA and GSK126 alone or in combination by western blotting analysis (left panel: gel bands; right panel: quantitative analysis of these proteins). **b** The effect of OCA and GSK126 on the nuclear translocation of FXR detected by IF staining. **c, d, e** The effect of CDX2 depletion on the growth (c), colony formation (d left panel: colony formation assays; right panel: quantitation of the data) and cell cycle distribution (e left panel: cell cycle analysis assays; right panel: quantitation of the data) of HCT116 and SW480 cells treated with OCA and GSK126 alone or in combination. **f, g** The effect of CDX2 depletion on the migration (f left panel: wound-healing assays; right panel: quantitation of the data) and invasion (g left panel: transwell assays; right panel: quantitation of the data) of HCT116 and SW480 cells treated with OCA and GSK126 alone or in combination. All data are the mean \pm SD of three independent experiments. * P < 0.05.

supports a close relevance between EZH2 expression and human malignancies, for instance that of EZH2 was highly expressed in bladder [39], breast [40], endometrial [41], and prostate cancer [42] correlating with tumor progression. In this study, we revealed that FXR expression was silenced by EZH2 through H3K27m3 modification. Additionally, dysfunction of APC mediates FXR silencing through CpG hypermethylation of the FXR promoter region [11]. Collectively, the combination therapy based on targeting FXR and its regulatory mechanism could be a very rational and promising treatment of CRC patients.

CDX2, drosophila caudal-related homoeobox transcription factor, is an intestine-specific transcriptional factor implicated in the intestinal development and maintenance [43]. Several lines of evidences support that CDX2 is a tumor suppressor in CRC. The deficiency of CDX2 increases colorectal cancer susceptibility [44]. Our data revealed that enhancing CDX2 expression blocks tumor progression and retards liver metastasis in CRC [29, 45]. Mechanistically, CDX2 repressed epithelial-mesenchymal transition (EMT) in CRC by regulating Snail expression and β -Catenin stabilization via transcriptionally activating PTEN [29]. In this study, the IR-1 site

was identified in the promoter fragments of CDX2. Moreover, the dual-luciferase reporter assay and qChIP assays demonstrated that FXR bound to the IR-1 site in the promoter region of CDX2 and induced CDX2 transcription. Our study for the first time revealed that CDX2 is directly regulated by FXR via transcriptional activation. Intriguingly, Modica et al identified CDX2 as a positive regulator of FXR expression in intestinal cells [46], implying that there might exist CDX2-FXR reciprocal regulation in colorectal tumorigenesis. Collectively, our study identified FXR as a novel mediator of CDX2 expression.

Additionally, the combination of OCA plus GSK126 synergistically elevated CDX2 expression in colon cancer cells and their derived xenograft tumor, compared to the single drug. The elevation of CDX2 might be attributed the upregulation of FXR and the accelerative nuclear localization of FXR, as demonstrated in this study. Correspondingly, the combination treatment triggered CDX2 regulatory pathway with the retardation of phosphorylation of Akt and GSK-3 β and nuclear translocation of β -Catenin [29]. The expression of p21, E-cadherin, and active caspase-3 were upregulated, and the expression of cyclin D1,

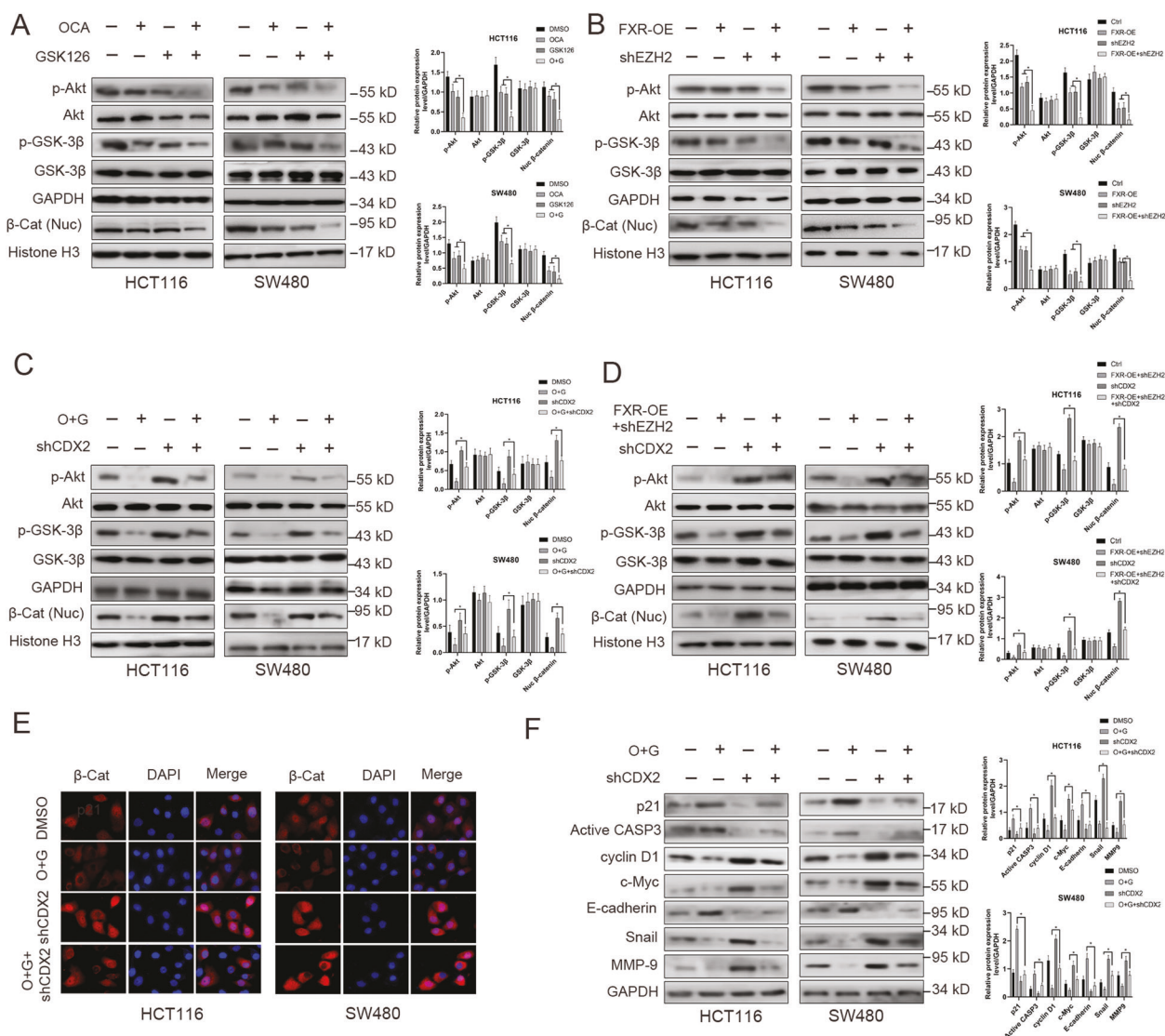


Fig. 5 The combination of OCA and GSK126 synergistically accelerated FXR nuclear localization and promoted CDX2 expression and its regulated signaling pathways. a The protein levels of AKT/p-AKT (Ser473), GSK-3β/p-GSK-3β (Ser9), and β-Catenin (Nuclear) in HCT116 and SW480 cells treated with OCA and GSK126 alone or in combination by western blotting analysis (left panel: gel bands; right panel: quantitative analysis of these proteins). **b** The protein levels of AKT/p-AKT (Ser473), GSK-3β/p-GSK-3β (Ser9) and β-Catenin (Nuclear) in HCT116 and SW480 cells with FXR overexpression, EZH2 depletion alone or in combination by western blotting analysis (left panel: gel bands; right panel: quantitative analysis of these proteins). **c, d** The effect of CDX2 depletion on the he protein levels of AKT/p-AKT (Ser473), GSK-3β/p-GSK-3β (Ser9), and β-Catenin (Nuclear) in HCT116 and SW480 with OCA and GSK126 combination (**c** left panel: gel bands; right panel: quantitative analysis of these proteins) or FXR overexpression and EZH2 depletion (**d** left panel: gel bands; right panel: quantitative analysis of these proteins). **e** The effect of OCA and GSK126 on the nuclear translocation of β-Catenin detected by IF staining. **f** The effect of CDX2 depletion on the protein levels of cell cycle-related, apoptosis-related, and EMT-related proteins in HCT116 and SW480 cells treated with OCA and GSK126 alone or in combination by western blotting analysis (left panel: gel bands; right panel: quantitative analysis of these proteins). All data are the mean ± SD of three independent experiments. *P < 0.05.

c-Myc, Snail, and MMP-9 was downregulated upon the drug combination.

Monoclonal antibodies against epidermal growth factor receptor (EGFR) or vascular endothelial growth factor (VEGF) have been entered the therapeutic regimen of metastatic CRC treatment. However, the effectiveness of EGFR inhibitor is constrained by intrinsic drug resistance due to KRAS mutations [47]. Intriguingly, Chen et al. reported that combined treatment of β-elemene and cetuximab elicited a synergistic antitumor effect on KRAS mutant CRC cells by induction of ferroptosis [48]. Given that the critical role of c-Src kinase in the intricate mechanisms of resistance to EGFR inhibitor, c-Src inhibitors in combination with EGFR inhibitors are at the stage of pre-clinical phase [49]. Hence,

combination therapy based on monoclonal antibodies might offers an innovative and effective strategy for CRC patients with RAS mutations. The vital role of EZH2 in tumorigenesis highlight targeting EZH2 as a promising therapeutic strategy in cancer treatment. Multiple kinds of EZH2 inhibitor have been developed, and several clinical trials of target EZH2 for different cancer types are ongoing. GSK126 is a highly selective and potent inhibitor of EZH2. Recently, a phase I study revealed a modest anticancer effect of GSK126 on human hematologic and solid tumors, despite that drug administration and relatively short half-life limited effective exposure [50]. Combining EZH2 inhibitors with target therapy might improve the treatment efficacy and overcome the limitation of monotherapy. Co-inhibition of both EZH2 and EGFR

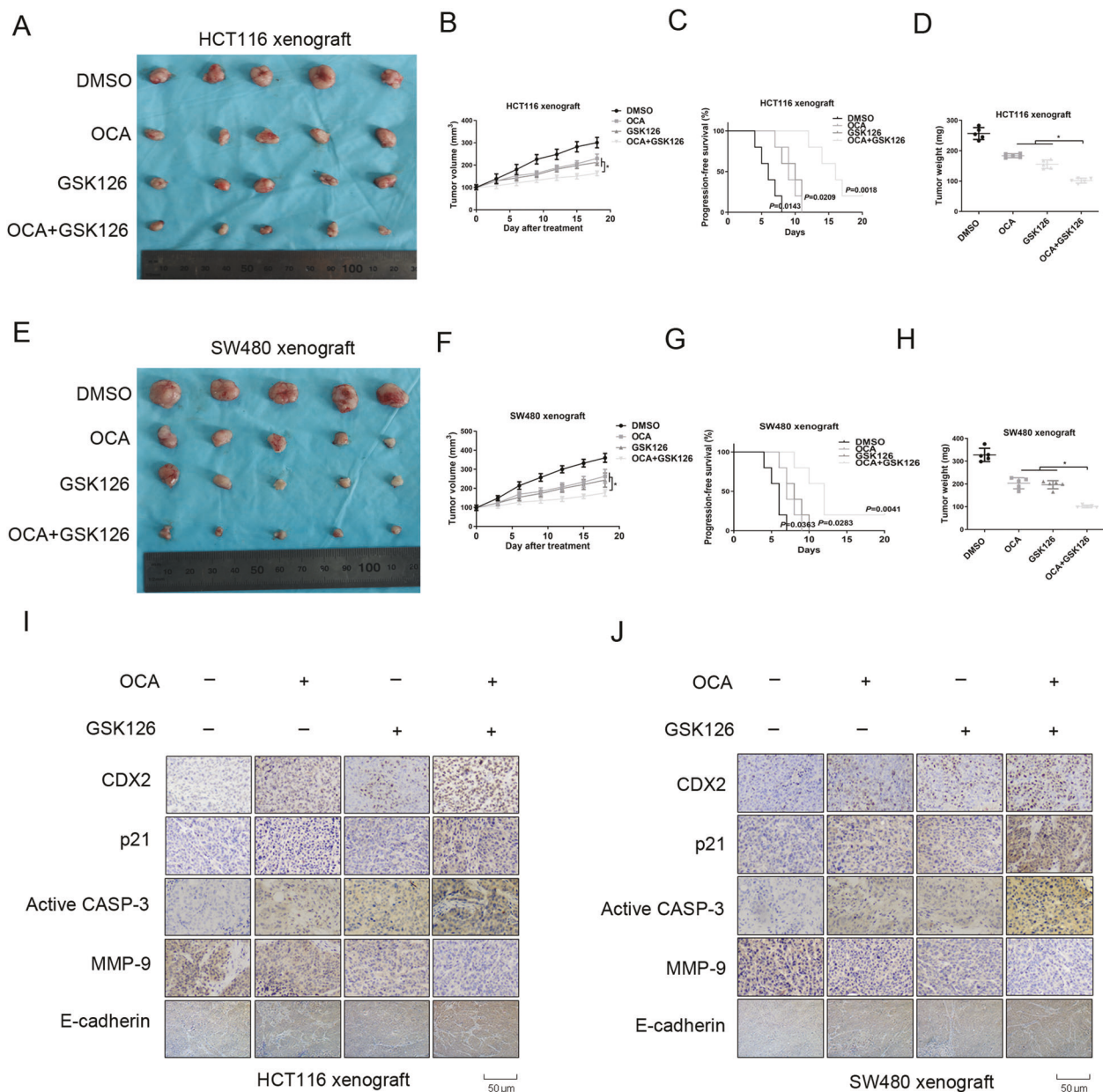


Fig. 6 OCA and GSK126 synergistically retarded tumor growth in vivo. **a, e** Schematic representation of the tumor xenografts formed by HCT116 (**a**) and SW480 (**e**) cells treated with OCA, GSK126 alone or OCA plus GSK126. **b, d, f, h** Tumor growth curves (**b, f**) and tumor weights (**d, h**) for tumor xenograft formed by HCT116 and SW480 cells after OCA, GSK126 alone, or OCA plus GSK126 treatment. **c, g** Cumulative incidence plot displaying the percentage of tumor xenografts formed by HCT116 (**c**) and SW480 (**g**) cells in each treatment group that has doubled in volume as a function of time. *P* values were calculated with log-rank test. **i, j** IHC staining for CDX2, p21, active caspase-3, MMP-9, and E-cadherin in tumor xenografts formed by HCT116 (**i**) and SW480 (**j**) cells. **P* < 0.05.

elicited a synergic effect on tumor growth suppression in CRC by triggering autophagy and inducing apoptosis [51]. Our previous study revealed that that colon cancer cells exhibited the varying responses to OCA [16]. Herein, we identified the EZH2 inhibitor GSK126 with synergism with FXR agonist OCA in confronting CRC. The combination treatment thoroughly inhibited the aggressive phenotype of the four colon cancer cells by a series of in vitro and in vivo experiments. The combination treatment overcame the varied responses of four colon cancer cells to OCA. More importantly, the combined treatment had low toxic side effects for normal epithelial cells. Mechanistically, our study revealed that this synergistic effect was probably attributed to the acceleration of FXR nuclear location and the upregulation of CDX2 expression.

However, the therapeutic effects of combination therapy require further evaluation in clinical trials, and the side effects and patient tolerance might limit the effectiveness.

Collectively, the present study for the first time demonstrated that the expression of FXR was positively correlated with EZH2 in colon cancer tissues. EZH2 transcriptionally suppressed FXR via H3K27me3, which subsequently activated the expression of tumor suppressor CDX2. The combination of FXR agonist plus EZH2 inhibitor exerts synergistic tumor inhibition in CRC both in vitro and in vivo by dramatically accelerating FXR nuclear location and cooperatively upregulating CDX2 expression. Our study offers useful evidence for the clinical use of FXR agonists combined with EZH2 inhibitors in combating CRC.

DATA AVAILABILITY

All data needed to evaluate the conclusions in the paper are present in the paper. Additional data related to this paper may be requested from the corresponding author.

REFERENCES

1. Coppede F, Lopomo A, Spisni R, Migliore L. Genetic and epigenetic biomarkers for diagnosis, prognosis and treatment of colorectal cancer. *World J Gastroenterol.* 2014;20:943–56.
2. Mei Z, Liu Y, Liu C, Cui A, Liang Z, Wang G, et al. Tumour-infiltrating inflammation and prognosis in colorectal cancer: systematic review and meta-analysis. *Br J Cancer.* 2014;110:1595–605.
3. Brenner H, Kloor M, Pox CP. Colorectal cancer. *Lancet.* 2014;383:1490–502.
4. Keum N, Giovannucci E. Global burden of colorectal cancer: emerging trends, risk factors and prevention strategies. *Nat Rev Gastroenterol Hepatol.* 2019;16:713–32.
5. Müller MF, Ibrahim AE, Arends MJ. Molecular pathological classification of colorectal cancer. *Virchows Arch.* 2016;469:125–34.
6. Gadaleta RM, Garcia-Irigoyen O, Moschetta A. Bile acids and colon cancer: Is FXR the solution of the conundrum? *Mol Asp Med.* 2017;56:66–74.
7. Rosignoli P, Fabiani R, De Bartolomeo A, Fuccelli R, Pelli MA, Morozzi G. Genotoxic effect of bile acids on human normal and tumour colon cells and protection by dietary antioxidants and butyrate. *Eur J Nutr.* 2008;47:301–9.
8. Chen ML, Takeda K, Sundrud MS. Emerging roles of bile acids in mucosal immunity and inflammation. *Mucosal Immunol.* 2019;12:851–61.
9. Moschetta A, Portincasa P, van Erpecum KJ, Debellis L, Vanberge-Henegouwen GP, Palasciano G. Sphingomyelin protects against apoptosis and hyperproliferation induced by deoxycholate: potential implications for colon cancer. *Dig Dis Sci.* 2003;48:1094–101.
10. Chavez-Talavera O, Tailleux A, Lefebvre P, Staels B. Bile acid control of metabolism and inflammation in obesity, type 2 diabetes, dyslipidemia, and nonalcoholic fatty liver disease. *Gastroenterology.* 2017;152:1679–94.e1673.
11. Selmin OL, Fang C, Lyon AM, Doetschman TC, Thompson PA, Martinez JD, et al. Inactivation of adenomatous polyposis coli reduces bile acid/farnesoid X receptor expression through Fxr gene CpG methylation in mouse colon tumors and human colon cancer cells. *J Nutr.* 2016;146:236–42.
12. Li S, Xu Z, Guo J, Zheng J, Sun X, Yu J. Farnesoid X receptor activation induces antitumour activity in colorectal cancer by suppressing JAK2/STAT3 signalling via transactivation of SOCS3 gene. *J Cell Mol Med.* 2020;24:14549–60.
13. Attia YM, Tawfiq RA, Ali AA, Elmazar MM. The FXR agonist, obeticholic acid, suppresses HCC proliferation & metastasis: role of IL-6/STAT3 signalling pathway. *Sci Rep.* 2017;7:12502.
14. Erice O, Labiano I, Arbelaitz A, Santos-Laso A, Munoz-Garrido P, Jimenez-Agüero R, et al. Differential effects of FXR or TGR5 activation in cholangiocarcinoma progression. *Biochim Biophys Acta.* 2018;1864:1335–44.
15. Thompson MD, Moghe A, Cornuet P, Marino R, Tian J, Wang P, et al. beta-Catenin regulation of farnesoid X receptor signaling and bile acid metabolism during murine cholestasis. *Hepatology.* 2018;67:955–71.
16. Yu J, Yang K, Zheng J, Zhao W, Sun X. Synergistic tumor inhibition of colon cancer cells by nitazoxanide and obeticholic acid, a farnesoid X receptor ligand. *Cancer Gene Ther.* 2020;28:590–601.
17. Ohno T, Shirakami Y, Shimizu M, Kubota M, Sakai H, Yasuda Y, et al. Synergistic growth inhibition of human hepatocellular carcinoma cells by acyclic retinoid and GW4064, a farnesoid X receptor ligand. *Cancer Lett.* 2012;323:215–22.
18. Nguyen LH, Goel A, Chung DC. Pathways of colorectal carcinogenesis. *Gastroenterology.* 2020;158:291–302.
19. Duan R, Du W, Guo W. EZH2: a novel target for cancer treatment. *J Hematol Oncol.* 2020;13:104.
20. Li L, Liu J, Xue H, Li C, Liu Q, Zhou Y, et al. A TGF-β-MTA1-SOX4-EZH2 signaling axis drives epithelial-mesenchymal transition in tumor metastasis. *Oncogene.* 2020;39:2125–39.
21. Huang KB, Zhang SP, Zhu YJ, Guo CH, Yang M, Liu J, et al. Hotair mediates tumorigenesis through recruiting EZH2 in colorectal cancer. *J Cell Biochem.* 2019;120:6071–7.
22. Singh AK, Verma A, Singh A, Arya RK, Maheshwari S, Chaturvedi P, et al. Salinomycin inhibits epigenetic modulator EZH2 to enhance death receptors in colon cancer stem cells. *Epigenetics.* 2020;16:1–18.
23. Yu J, Liu D, Sun X, Yang K, Yao J, Cheng C, et al. CDX2 inhibits the proliferation and tumor formation of colon cancer cells by suppressing Wnt/beta-catenin signaling via transactivation of GSK-3β and Axin2 expression. *Cell Death Dis.* 2019;10:26.
24. Yu J, Li S, Qi J, Chen Z, Wu Y, Guo J, et al. Cleavage of GSDME by caspase-3 determines lobaplatin-induced pyroptosis in colon cancer cells. *Cell Death Dis.* 2019;10:193.
25. Su H, Ma C, Liu J, Li N, Gao M, Huang A, et al. Downregulation of nuclear receptor FXR is associated with multiple malignant clinicopathological characteristics in human hepatocellular carcinoma. *Am J Physiol Gastrointest Liver Physiol.* 2012;303:G1245–53.
26. Yu J, Li S, Guo J, Xu Z, Zheng J, Sun X. Farnesoid X receptor antagonizes Wnt/β-catenin signaling in colorectal tumorigenesis. *Cell Death Dis.* 2020;11:640.
27. Yu JH, Zheng JB, Qi J, Yang K, Wu YH, Wang K, et al. Bile acids promote gastric intestinal metaplasia by upregulating CDX2 and MUC2 expression via the FXR/NF-κB signalling pathway. *Int J Oncol.* 2019;54:879–92.
28. Zhou J, Cui S, He Q, Guo Y, Pan X, Zhang P, et al. SUMOylation inhibitors synergize with FXR agonists in combating liver fibrosis. *Nat Commun.* 2020;11:240.
29. Yu J, Li S, Xu Z, Guo J, Li X, Wu Y, et al. CDX2 inhibits epithelial-mesenchymal transition in colorectal cancer by modulation of Snail expression and β-catenin stabilisation via transactivation of PTEN expression. *Br J Cancer.* 2021;124:270–80.
30. Jin ZJ. Addition in drug combination (author's transl). *Zhongguo Yao Li Xue Bao.* 1980;1:70–6.
31. Finn RS. Emerging targeted strategies in advanced hepatocellular carcinoma. *Semin Liver Dis.* 2013;33:S11–9.
32. Chiang JYL, Ferrell JM. Bile acid receptors FXR and TGR5 signaling in fatty liver diseases and therapy. *Am J Physiol Gastrointest Liver Physiol.* 2020;318:G554–73.
33. Sun L, Xie C, Wang G, Wu Y, Wu Q, Wang X, et al. Gut microbiota and intestinal FXR mediate the clinical benefits of metformin. *Nat Med.* 2018;24:1919–29.
34. Lee JY, Lee KT, Lee JK, Lee KH, Jang KT, Heo JS, et al. Farnesoid X receptor, overexpressed in pancreatic cancer with lymph node metastasis promotes cell migration and invasion. *Br J Cancer.* 2011;104:1027–37.
35. Guan B, Li H, Yang Z, Hoque A, Xu X. Inhibition of farnesoid X receptor controls esophageal cancer cell growth in vitro and in nude mouse xenografts. *Cancer.* 2013;119:1321–9.
36. Wolfe A, Thomas A, Edwards G, Jaseja R, Guo GL, Apté U. Increased activation of the Wnt/β-catenin pathway in spontaneous hepatocellular carcinoma observed in farnesoid X receptor knockout mice. *J Pharm Exp Ther.* 2011;338:12–21.
37. Fu T, Coulter S, Yoshihara E, Oh TG, Fang S, Cayabyab F, et al. FXR regulates intestinal cancer stem cell proliferation. *Cell.* 2019;176:1098–112.e1018.
38. Di Croce L, Helin K. Transcriptional regulation by polycomb group proteins. *Nat Struct Mol Biol.* 2013;20:1147–55.
39. Ramakrishnan S, Granger V, Rak M, Hu Q, Attwood K, Aquila L, et al. Inhibition of EZH2 induces NK cell-mediated differentiation and death in muscle-invasive bladder cancer. *Cell Death Differ.* 2019;26:2100–14.
40. Anwar T, Arellano-Garcia C, Ropa J, Chen YC, Kim HS, Yoon E, et al. p38-mediated phosphorylation at T367 induces EZH2 cytoplasmic localization to promote breast cancer metastasis. *Nat Commun.* 2018;9:2801.
41. Krill L, Deng W, Eskander R, Mutch D, Zweizig S, Hoang B, et al. Overexpression of enhance of Zeste homolog 2 (EZH2) in endometrial carcinoma: an NRG Oncology/Gynecologic Oncology Group Study. *Gynecol Oncol.* 2020;156:423–9.
42. Varambally S, Dhanasekaran SM, Zhou M, Barrette TR, Kumar-Sinha C, Sanda MG, et al. The polycomb group protein EZH2 is involved in progression of prostate cancer. *Nature.* 2002;419:624–9.
43. Grainger S, Savory JG, Lohnes D. Cdx2 regulates patterning of the intestinal epithelium. *Dev Biol.* 2010;339:155–65.
44. Aoki K, Kakizaki F, Sakashita H, Manabe T, Aoki M, Taketo MM. Suppression of colonic polyposis by homeoprotein CDX2 through its nontranscriptional function that stabilizes p27kip1. *Cancer Res.* 2011;71:593–602.
45. Yu J, Liu D, Sun X, Yang K, Yao J, Cheng C, et al. CDX2 inhibits the proliferation and tumor formation of colon cancer cells by suppressing Wnt/β-catenin signaling via transactivation of GSK-3β and Axin2 expression. *Cell Death Dis.* 2019;10:26.
46. Modica S, Cariello M, Morgano A, Grossi I, Vegliante MC, Murzilli S, et al. Transcriptional regulation of the intestinal nuclear bile acid farnesoid X receptor (FXR) by the caudal-related homeobox 2 (CDX2). *J Biol Chem.* 2014;289:28421–32.
47. Dunn EF, Iida M, Myers RA, Campbell DA, Hintz KA, Armstrong EA, et al. Dasatinib sensitizes KRAS mutant colorectal tumors to cetuximab. *Oncogene.* 2011;30:561–74.
48. Chen P, Li X, Zhang R, Liu S, Xiang Y, Zhang M, et al. Combinative treatment of β-elemene and cetuximab is sensitive to KRAS mutant colorectal cancer cells by inducing ferroptosis and inhibiting epithelial-mesenchymal transformation. *Theranostics.* 2020;10:5107–19.
49. Belli S, Esposito D, Servetto A, Pesapane A, Formisano L, Bianco R. c-Src and EGFR inhibition in molecular cancer therapy: What else can we improve? *Cancers.* 2020;12:1489.
50. Yap TA, Winter JN, Giulino-Roth L, Longley J, Lopez J, Michot JM, et al. Phase I study of the novel enhancer of zeste homolog 2 (EZH2) inhibitor GSK2816126 in patients with advanced hematologic and solid tumors. *Clin Cancer Res.* 2019;25:7331–9.
51. Katona BW, Liu Y, Ma A, Jin J, Hua X. EZH2 inhibition enhances the efficacy of an EGFR inhibitor in suppressing colon cancer cells. *Cancer Biol Ther.* 2014;15:1677–87.

ACKNOWLEDGEMENTS

This work was funded by a grant from the National Natural Science Foundation of China (Grant Serial Numbers: 81972720, 82002547, and 81973238).

AUTHOR CONTRIBUTIONS

J.H.Y. and K.Y. performed the experiments, acquired data, and drafted the article. All authors revised the article critically for important intellectual content. J.B.Z. and J.X. analyzed and interpreted data. W.Z. and P.W.Z. collected the clinical samples and evaluated all specimens. X.J.S. and W.Z. substantially contributed to conception and design. All authors read and approved the final manuscript and agreed to be accountable for all aspects of the research in ensuring that the accuracy or integrity of any part of the work are appropriately investigated and resolved.

ETHICS APPROVAL

All animal experiments in our study were carried out in accordance with the Helsinki Declaration, and approved by the Ethics Committee of The First Affiliated Hospital of Xi'an Jiaotong University. Patients were informed that the resected specimens were stored by the hospital and potentially used for scientific research, and that their privacy would be maintained. All patients provided informed consent prior to undergoing surgery. Our study protocol was approved by the Ethics Committee of the First Affiliated Hospital of Xi'an Jiaotong University.

COMPETING INTERESTS

The authors declare no competing interests.

ADDITIONAL INFORMATION

Supplementary information The online version contains supplementary material available at <https://doi.org/10.1038/s41419-022-04745-5>.

Correspondence and requests for materials should be addressed to Jie Xia, Xuejun Sun or Wei Zhao.

Reprints and permission information is available at <http://www.nature.com/reprints>

Publisher's note Springer Nature remains neutral with regard to jurisdictional claims in published maps and institutional affiliations.



Open Access This article is licensed under a Creative Commons Attribution 4.0 International License, which permits use, sharing, adaptation, distribution and reproduction in any medium or format, as long as you give appropriate credit to the original author(s) and the source, provide a link to the Creative Commons license, and indicate if changes were made. The images or other third party material in this article are included in the article's Creative Commons license, unless indicated otherwise in a credit line to the material. If material is not included in the article's Creative Commons license and your intended use is not permitted by statutory regulation or exceeds the permitted use, you will need to obtain permission directly from the copyright holder. To view a copy of this license, visit <http://creativecommons.org/licenses/by/4.0/>.

© The Author(s) 2022, corrected publication 2023